Paleoceanography and Paleoclimatology

RESEARCH ARTICLE
10.1029/2019PA003738

Planktic Foraminiferal Test Size and Weight Response to the Late Pliocene Environment

C. L. Todd[1], D. N. Schmidt[1], M. M. Robinson[2], and S. De Schepper[3]

[1]School of Earth Sciences, University of Bristol, Bristol, UK, [2]Florence Bascom Geoscience Center, U.S. Geological Survey, Reston, VA, USA, [3]Bjerknes Centre for Climate Research, NORCE Norwegian Research Centre, Bergen, Norway

Key Points:
- Size in foraminiferal assemblages during the late Pliocene is smaller than modern at the same environmental conditions
- Size in planktic foraminifera depends on environment and changes through time, with temperature and stratification being the main controls
- Size-normalized weight during MIS M2 indicates multiple drivers of growth, calcification and density

Correspondence to:
C. L. Todd,
c.todd@bristol.ac.uk

Citation:
Todd, C. L., Schmidt, D. N., Robinson, M. M., & De Schepper, S. (2020). Planktic foraminiferal test size and weight response to the late Pliocene environment. *Paleoceanography and Paleoclimatology*, *35*, e2019PA003738. https://doi.org/10.1029/2019PA003738

Received 25 JUL 2019
Accepted 23 DEC 2019
Accepted article online 02 JAN 2020

Abstract Atmospheric carbon dioxide (pCO_2^{atm}) is impacting the ocean and marine organisms directly via changes in carbonate chemistry and indirectly via a range of changes in physical parameters most dominantly temperature. To assess potential impacts of climate change on carbonate production in the open ocean, we measured size and weight of planktic foraminifers during the late Pliocene at pCO_2^{atm} concentrations comparable to today and global temperatures 2 to 3 °C warmer. Size of all foraminifers was measured at Atlantic Ocean Deep Sea Drilling Project (DSDP) Site 610, Ocean Drilling Program (ODP) Site 999, and Integrated Ocean Drilling Program (IODP) Site U1313. Test size was smaller during the Pliocene than in modern assemblages under the same environmental conditions. During the cold marine isotope stage (MIS) M2, size increased at Site 999, potentially linked to intensified stratification of the surface ocean in response to the closure of the Central American Seaway. At Site U1313, test size tracks the warming throughout the late Pliocene. Size-normalized weight (SNW) of *Globigerina bulloides* at Site U1313 decreased during warmer temperature intervals. SNW of *Globigerinoides ruber* (white) at Site 999 displays high-frequency variability not correlated to temperature. Yet during the glacial period within MIS M2, test weight was higher during higher temperatures. Our results support studies in the modern ocean, which challenge the view that carbonate chemistry is the primary driver for calcification. To better understand processes driving changes in SNW, computer tomography was used to quantify calcite to volume ratios. During interglacial periods, lower calcite volume but higher test volume suggests less suitable conditions for calcification. As this signal is not evident in SNW, subtle changes in calcification might not be observed by the weight-based method.

Plain Language Summary Calcium carbonate shell-producing organisms in the oceans are in danger of losing the ability to build shells because oceans are becoming warmer and more acidic from absorbing the excess carbon dioxide in the atmosphere. Here we measure the size and weight of microscopic plankton shells during a past climate interval about three million years ago when the atmospheric carbon dioxide level was similar to today. Studying this time interval allows us to quantify impacts of a warmer more acidic ocean on the ability of plankton in the ocean to produce carbonate. During this interval, temperature fluctuated, and local environmental conditions changed in response to the emergence of the Isthmus of Panama. We show here that both size and weight react to global and local drivers, which include but are not limited to temperature.

1. Introduction

Atmospheric carbon dioxide (pCO_2^{atm}) has increased from 280 parts per million (ppm) at the start of the industrial revolution (1750; Siegenthaler et al., 2005) to over 410 ppm today (2019; National Aeronautics and Space Administration, 2019). This increase in pCO_2^{atm} results in changes in the carbonate chemistry of the ocean, warming, increased stratification, and oxygen loss, all of which are projected to impact marine organisms (Pörtner et al., 2014).

Marine calcifying organisms play a fundamental role in the inorganic carbon cycle (Boyce et al., 2010; Henehan et al., 2017). Carbonate production in the ocean is roughly equally divided between the shelf and the open ocean (Cartapanis et al., 2018). In the open ocean ecosystem, planktic foraminifers are a significant sink for $CaCO_3$, producing 32 to 80 % of $CaCO_3$ flux to marine sediments (Schiebel, 2002). Therefore, any changes in their calcification in response to climate change could have impacts on the inorganic carbon cycle.

The amount of carbonate produced by an individual foraminifer is a function of the specimen's size and the thickness of the test. Growth of foraminiferal tests is regulated by several environmental factors including pH, temperature, salinity, light, oxygen, and nutrient levels, together with food availability (Kucera, 2007). Today, larger test sizes are generally found in the warm subtropical to tropical oceans with decreasing size toward the poles (de Villiers, 2004; Schmidt, Renaud, et al., 2004); trends across the group are the result of species-specific size. This pattern reflects the larger species diversity, and inclusion of relatively large species, in warmer subtropical and tropical waters. Within a single species, size is tied to optimum growth conditions, outside of which growth rates decrease and reproduction ceases (Schmidt et al., 2006; Schmidt, Renaud, et al., 2004). Increased test size in warmer surface waters has been related to a combination of carbonate saturation, faster metabolic rates, higher light intensity, and greater niche diversity due to stronger stratification (de Villiers, 2004; Lombard et al., 2009; Schmidt, Renaud, et al., 2004). As several of these factors are related to temperature, this suggests that temperature is the dominant control on growth in lower latitudes (Bijma et al., 1990) though the modern dataset does not allow to distinguish between temperature per se or stratification (Schmidt, Thierstein, Bollmann, & Schiebel, 2004). Modulating this overarching pattern, from oligotrophic to mesotrophic environments, increasing food facilitates growth to larger sizes until high productivity limits light to support symbiont bearing species, which are then replaced by smaller nonsymbiont bearing ones (Schmidt, Renaud, et al., 2004). Furthermore, sizes in highly changeable environments such as frontal systems and upwelling areas tend to be smaller than the general size temperature trend would suggest (Schmidt, Renaud, et al., 2004).

Other than size, foraminiferal weight is a fundamental indicator of foraminiferal carbonate production. Planktic foraminifera in general respond to changes in lower pH, carbonate ion concentration, and saturation with thinner tests and reduction in test size (Barker & Elderfield, 2002; Bijma et al., 1999; Henehan et al., 2017; Naik et al., 2010; Spero et al., 1997). This calcification response is more prominent in nonsymbiotic foraminifera than in symbiotic species, which are able to elevate the pH in surrounding waters due to photosynthetic CO_2 fixation (de Nooijer et al., 2009; Rink et al., 1998; Wolf-Gladrow et al., 1999). The drivers of weight change in foraminifer are still heavily debated as some species and regions show no dependency on the carbonate system suggesting that temperature and productivity drive a change in calcification (Beer et al., 2010; Weinkauf et al., 2013; Weinkauf et al., 2016). For example, reduced salinity may inhibit calcification in some species of foraminifera (Beer et al., 2010; Bijma et al., 1990; Weinkauf et al., 2013).

We tested our understanding of the impact of climate change on foraminiferal carbonate production by analyzing size and weight at two sites during the late Pliocene (3.4 to 2.9 Ma) with reconstructed pCO_2 peaking at ~420 to 450 ppm (Dowsett & Gill, 2010; Martínez-Botí et al., 2015; Pagani et al., 2010; Seki et al., 2010). The Pliocene ocean had similar circulation and faunal distribution to modern (Robinson et al., 2008) and therefore is an ideal test interval for this comparison (Dowsett et al., 2012; Haywood et al., 2013). Global sea surface temperature (SST) is estimated to have been 2 to 3 °C higher, surface pH ~0.06 to 0.11 units lower, and sea level ~25 m above current levels (Dowsett et al., 2012; Dwyer & Chandler, 2009; Haywood et al., 2016; Hönisch et al., 2012; Miller et al., 2012; Robinson et al., 2008). The predominantly warm late Pliocene was interrupted by a short-lived glaciation (3.285 to 3.305 Ma) within marine isotope stage (MIS) M2 (3.26 to 3.31 Ma; De Schepper et al., 2013; Dowsett et al., 2015). MIS M2 may have been a response to the closure of the Central American Seaway (CAS; De Schepper et al., 2013; Karas et al., 2017); changes in pCO_2 also likely played an important role (Tan et al., 2017). Unfortunately, no high resolution pCO_2 records across MIS M2 currently exist to offer further insight into this question.

At Sites 610, 999, and U1313, we measure the size of all specimens within the late Pliocene assemblages and determine size-normalized weight (SNW) of *Globigerinoides ruber* (white) in the Caribbean Sea (Site 999) and *Globigerina bulloide*s in the North Atlantic Ocean (Site U1313). These species were chosen due to their high abundance in the assemblage at each location to asses if smaller size is associated with thinner tests in response to the higher atmospheric pCO_2 in the late Pliocene. To interpret any changes in SNW, we used microcomputer tomography to measure changes in thickness and calcite on each specimen.

Our previous work suggests competing impacts on assemblage size of evolutionary tendency for larger size in the most modern icehouse assemblages (Schmidt, Thierstein, Bollmann, & Schiebel, 2004), while

ecological drivers result in largest sizes in highly stratified warm waters today (Schmidt, Renaud, et al., 2004). Consequently, low-resolution studies suggest that the size in foraminiferal assemblages is lower during the Pliocene than today (Schmidt, Thierstein, & Bollmann, 2004), and therefore, we are expecting smaller sizes compared to modern. Therefore, supported by research on glacial-interglacial variability (Barker & Elderfield, 2002; Schmidt et al., 2003), we would expect the Pliocene assemblages to be overall smaller than modern and smallest during M2. Based on laboratory studies and sediment samples, the expectation is that in a warmer world with higher pCO_2^{atm}, the weight of individuals should be lower, compared to modern (Barker & Elderfield, 2002; Bijma et al., 2002). The growth and calcification response should be largest in regions of the ocean where the environment varies most between glacial and interglacial intervals (e.g., higher latitudes) and smaller in regions with lower amplitudes of change (e.g., lower latitudes; Renaud & Schmidt, 2003; Schmidt et al., 2003).

2. Materials and Methods

2.1. Materials

We analyzed planktic foraminifers from Ocean Drilling Program (ODP) Site 999, Integrated Ocean Drilling Program (IODP) Site U1313, and Deep Sea Drilling Project (DSDP) Site 610 to form a transect from the tropical to higher latitude Atlantic Ocean. ODP Site 999 (12°44″N, 78°44′W, 2,828 m water depth; Sigurdsson et al., 1996; Figure 1) is located in the Caribbean Sea. Hole 999A is predominantly composed of nannofossil clayey mixed sediments with foraminifers and foraminiferal clayey mixed sediment with nannofossils (Sigurdsson et al., 1996). We adopt the age model of Groeneveld (2005), which was initially established by Haug and Tiedemann (1998b). Sedimentation rate during the late Pliocene was 3.0 to 3.3 cm/kyr (Sigurdsson et al., 1996). One hundred thirty-four samples over 419 kyr were analyzed, resulting in an average temporal resolution of 3.1 kyr.

Site U1313 is situated at the base of the upper western flank of the mid-Atlantic Ridge (41°0′N, 32°57′W) in a water depth of 3,413 m (Channell et al., 2006; Figure 1). The core material consists of a carbonate nannofossil ooze, with less than 5 % clay (Channell et al., 2006). The age model is based on De Schepper et al. (2013) and Naafs et al. (2010). The sedimentation rate was 4.1 to 4.5 cm/kyr throughout the late Pliocene (Channell et al., 2006). One hundred twenty-four samples, from both Holes U1313B and U1313C, over 212 kyr were used with an average temporal resolution of 1.7 kyr.

Hole 610A was cored in the northern North Atlantic Ocean (53°13′N, 18°53′W; Figure 1) at a water depth of 2,417 m (Ruddiman et al., 1983) and is composed of cyclic alternations of pelagic sediments with glacial mud and interglacial nannofossil ooze (Ruddiman et al., 1983). We use the age model from the initial site report (Ruddiman et al., 1983) suggesting a sedimentation rate of 5.1 cm/kyr (Ruddiman et al., 1983). Sixteen samples over 87 kyr, with a temporal resolution of 5.4 cm/kyr, were used in the determination of latitudinal size gradients in the late Pliocene.

We incorporate Mg/Ca SST estimates, measured on *Trilobatus sacculifer*, from Groeneveld (2005) at Hole 999A, with a resolution of 6 kyr and compare to the alkenone temperature record with a resolution of 13 kyr (Bartoli et al., 2011; Martínez-Botí et al., 2015). The alkenone temperature record has been to complement the Mg/Ca SST as this record might be biased toward lower temperatures at Site 999 due to dissolution as indicated by fragmentation. We use the Site U1313 Mg/Ca temperature record, measured on *G. bulloides*, from De Schepper et al. (2013), with a resolution of 2 kyr and compare to the alkenone temperature record with a resolution of 4 kyr (De Schepper et al., 2013). The *G. bulloides* Mg/Ca SST record for Hole 610A is also taken from De Schepper et al. (2013). The LR04 benthic foraminifera oxygen isotope stack (Lisiecki & Raymo, 2005) has been used to correlate the samples. As no high-resolution atmospheric CO_2 (pCO_2^{atm} [ppm]) data exist for these sites, we use the boron isotope data from Martínez-Botí et al. (2015) and Bartoli et al. (2011) to provide information on pH changes.

2.2. Methods

2.2.1. Assemblage size Analysis

Sediment samples from Sites 999, U1313, and 610 were washed over a 63 μm sieve and dry-sieved at 150 μm. Planktic foraminiferal assemblage size was determined through the analysis of community size generated by automated microscopy (Bollmann et al., 2004; Schmidt, Renaud, et al., 2004). The samples were split

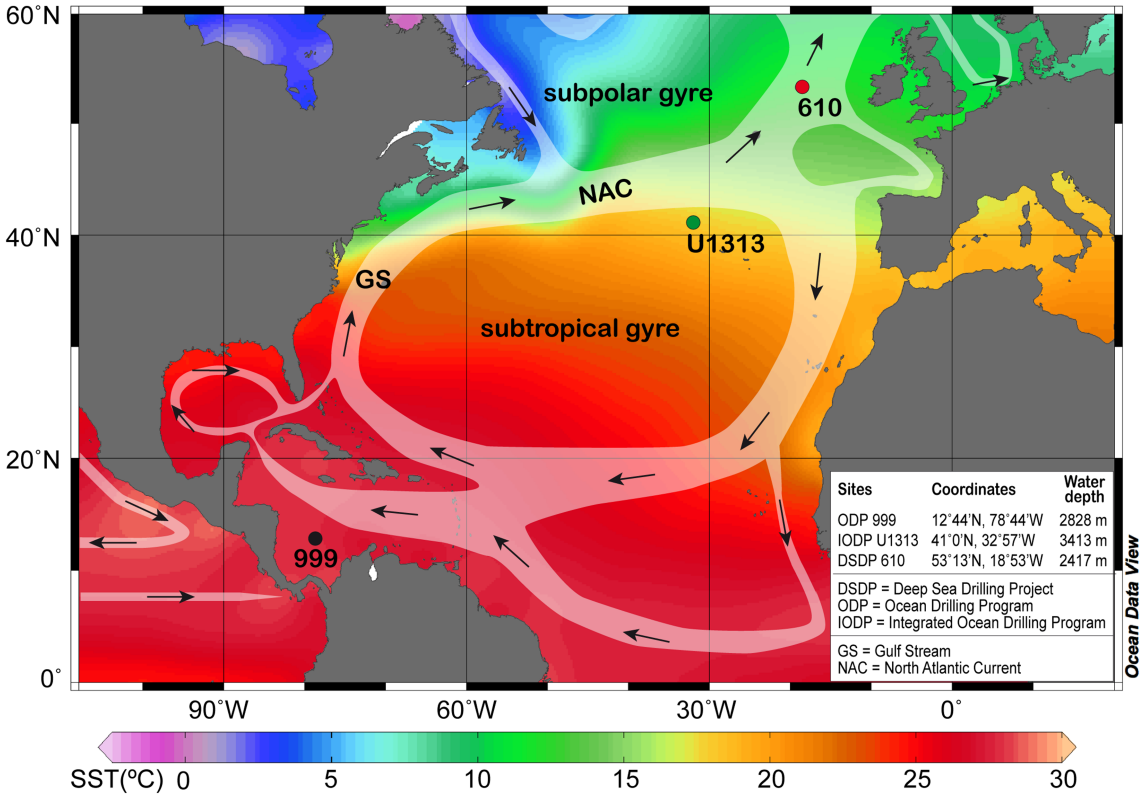

Figure 1. Location map of Ocean Drilling Program (ODP) Site 999, Deep Sea Drilling Project (DSDP) Site 610, and Integrated Ocean Drilling Program (IODP) Site U1313 (adapted from De Schepper et al., 2013). Arrows are showing the modern surficial currents and sea surface temperature.

representatively using a microsplitter so that ~800 to ~3,000 specimens of each sample were photographed at a magnification of 160x following Schmidt, Thierstein, and Bollmann (2004). Morphological parameters were analyzed using Olympus Stream Motion. Parameters were set to exclude particles with a maximum diameter below 150 μm, below sphericity of 0.5, and below the mean grey value of 40; the particles outside these thresholds represent broken foraminifers, other microfossils, and rock fragments such as ice rafted debris or volcanic ash. Benthic foraminifera, ostracods, diatoms, and other material were removed through manual assessment of the images with the largest particle size to avoid bias in the data. The 95th percentile of the maximum diameter was calculated on the remaining data, following the method of Schmidt, Renaud, et al. (2004) as the differences between the size spectra of the assemblages are predominantly changing the skewness of the distribution. The average measurement error of the 95th percentile of the assemblage size (size$^{95/5}$) across both sites is 0.84 %, equal to 3.07 μm, and is therefore within the calculated accuracy of diameter measurements of 3.31 μm (Schmidt et al., 2003). The error was determined by the resplitting and repeat measurement of 51 samples.

2.2.2. Preservation

Currently, the lysocline is found at a depth between 4 and 5 km in the Atlantic Ocean (Thunnel, 1982) and in the Caribbean Sea (Archer, 1996), and hence, all sites are significantly above the carbonate compensation depth (Sigurdsson et al., 1996). In the Caribbean, during the Pliocene, the lysocline was deeper than today (Sigurdsson et al., 1996; Tiedemann & Franz, 1997) with potential impacts on size spectra in the assemblages; fragmentation is apparent in many samples.

Fragmentation can bias the assemblage size toward both higher and lower values by selectively removing more dissolution susceptible species, such as *Gs. ruber* and *Orbulina universa* (Berger, 1970) or by increasing the abundance of small fragments. To determine changes in carbonate preservation, fragmentation was counted in at least 200 particles of all samples, following the method of previous work on Pliocene samples from Sites 999 and U1313 (Davis et al., 2013) and the method by Le and Shackleton (1992). The ratio of broken versus complete foraminifers was calculated.

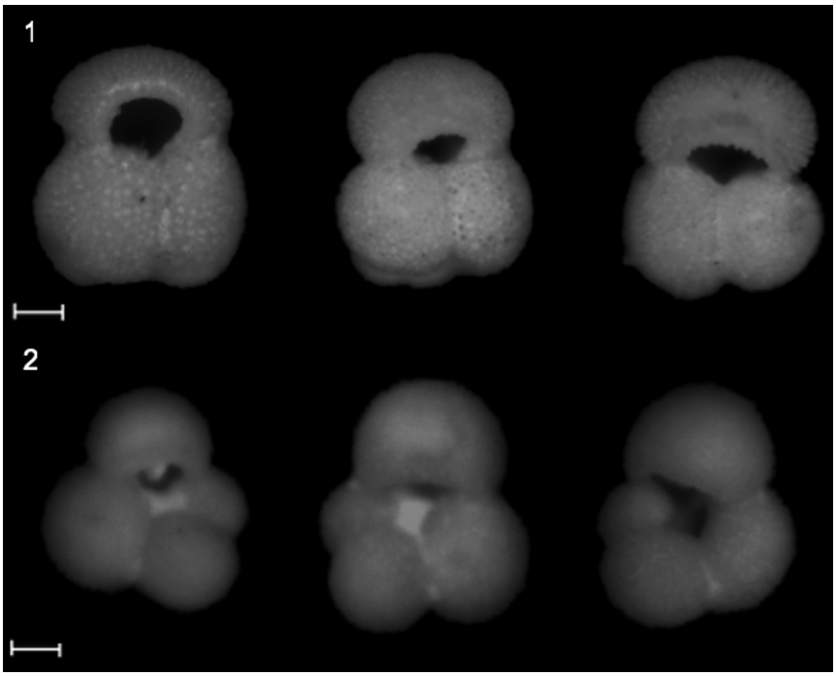

Figure 2. Examples of picked specimens used for size-normalized weight of (1) *Gs. ruber,* from Site 999 and (2) *G. bulloides*, from Site U1313. The scale bars represent 100 μm.

2.2.3. Size-Normalized Weight

To determine the SNW of foraminifera at ODP Site 999 through the Pliocene, 20 to 30 individuals of *Globigerinoides ruber* sensu stricto (Figure 2) were picked from the 300- to 355-μm size fraction of 86 samples following the method of Barker and Elderfield (2002). Other morphotypes are known to have different habitats (Aurahs et al., 2011), with *Gs. ruber* sensu lato (Figure 2) precipitating tests in colder surface waters than *Gs. ruber* sensu stricto (Steinke et al., 2005). For SNW of Site U1313 samples, 15 to 30 specimens of *G. bulloides* (Figure 2) were picked from the same size fraction for 48 samples, following the same method. There are several morphospecies of *G. bulloides* within which are genotypes that inhibit a range of ecologies (Darling & Wade, 2008). Based on the location of Site U1313, *G. bulloides* types IIa–IIe, with IIa and IIb likely to be dominant, are the genotypes present (Darling & Wade, 2008). There are no studies to show a morphological difference between these types. Samples were weighed to six-decimal places using a Mettler Toledo analytical balance to determine the average weight of the test (sieve-based weight). For every sample, the length of each specimen in the same orientation was taken from digital images using ImageJ. SNW for all samples was calculated by normalizing sieve-based weight to the mean diameter for the corresponding size following Barker and Elderfield (2002). Our data were combined with data from Davis et al. (2013), which was determined using the same method on the same instruments.

2.2.4. Microcomputer Tomography

To better interpret any changes in SNW, 15 of the *Gs. ruber* specimens that were used for SNW measurements (see section 2.2.3) were subsampled from four samples of Site 999, guided by the oxygen isotope ($\delta^{18}O$) record, to cover samples before, during and after MIS M2. Microcomputer tomographic images were taken using a Nikon XT H 225 ST CT scanner (120 kV, 58 Va), configured at 2.1- to 2.3 μm resolution, with an exposure time of 0.5 s and a total of 3,141 projections. These images were processed in Avizo 9.0 (Thermo Scientific™). The calcite test of the foraminifera is isolated from any infill to give the volume of the calcite (Figure 3). The internal cavity of each chamber (incorporating any infilling, to represent the true internal space) was manually isolated following Caromel et al. (2015) and Schmidt et al. (2016). External volume and volume of the calcite test were added to determine the volume of the foraminifera. The calcite to volume (CV) ratio was calculated (Figure 3). Due to the resolution of the scan, any change below 4 μm cannot be resolved with confidence. The method would also highlight any infilling with secondary calcite as a potential cause for weight changes.

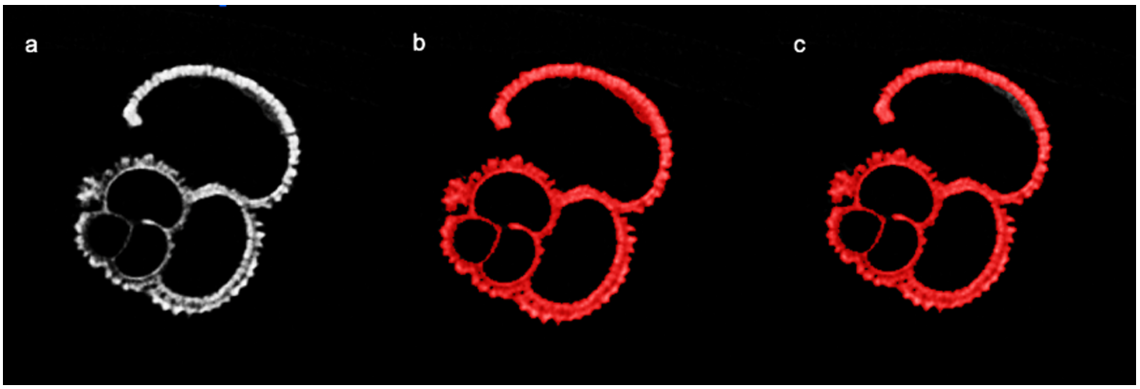

Figure 3. Microcomputer tomography tomographic process: (a) raw image of one layer from microcomputer tomography scans, (b) material selected, and (c) calcite test highlighted, after the removal of any other material.

3. Results

The fragmentation records of both sites show large-scale similarities. Fragmentation changes significantly between 15 and 60 % with poorer preservation (average fragmentation of 39.6 %) at Site 999 than at U1313 (average fragmentation 26.5 %; Figure 4b). Fragmentation decreases at Site 999 (but not at Site U1313) during MIS M2 suggesting a change in environmental conditions (Figure 4b). There is a weak correlation between fragmentation and Mg/Ca SST at 999 ($r = 0.22$, $P = 0.01$) but none at U1313 ($r = 0.12$, $P = 0.2$). Fragmentation and size are not correlated at both Site 999 ($r = -0.08$, $P = 0.34$) and Site U1313 ($r = 0.05$, $P = 0.55$).

Size$^{95/5}$ at Site 999 ranges from 386 to 551 μm (Figure 4a) and is not correlated with Mg/Ca temperature ($r = -0.15$, $P = 0.08$) or with alkenone SST ($r = -015$, $P = 0.48$). Regular peaks in size throughout the late Pliocene, on average every 43 kyr, show a focus on obliquity, which occurs every 41 kyr, but it may be modulated with precession, a 21-kyr cycle. Size$^{95/5}$ and SST track each other during MIS M2 ($r = -0.53$, $P < 0.01$) with larger sizes recorded at cooler temperatures but are not correlated before ($r = -0.15$, $P = 0.64$) or after MIS M2 ($r = 0.02$, $P = 0.85$). Overall both size$^{95/5}$ and pCO_2^{atm} are rather stable but not correlated (Figure 4f; $r = -0.05$, $P = 0.76$). It is important to note that the pCO_2^{atm} record is at a much lower resolution, in particular across MIS M2. There is very little variability of CO_2 within the precision of the data during and prior to MIS M2, questioning if CO_2 was the driver for the glaciation (Bartoli et al., 2011). At Site U1313, size$^{95/5}$ ranges from 290 to 444 μm (Figure 4a) and has a weak positive correlation with Mg/Ca SST ($r = 0.40$, $P < 0.001$), and no correlation to alkenone SST ($r = 0.24$, $P = 0.062$). In general, warming is associated with larger size throughout the Pliocene.

To determine latitudinal size gradients in comparison to the Holocene, size data were added at lower resolution from Site 610 (Figure 5). The low number of samples is only indicative of a trend in which colder temperatures lead to larger size. At Site 999 the average size is 464.1 μm ($SD = 33.76$ μm) and the average Mg/Ca temperature is 24 °C ($SD = 1.18$°C), with the average alkenone temperature being 28 °C ($SD = 0.25$ °C); at Site U1313 and Site 610 the size and temperature are 357 μm ($SD = 29.90$ μm) and 20 °C ($SD = 1.61$ °C) and 349 μm ($SD = 24.73$ μm) and 14 °C ($SD = 1.34$ °C), respectively (Figure 5). Overall, Pliocene foraminifer are smaller at the same temperature compared to the Holocene ($r = 0.91$, $P < 0.01$).

At Site 999, SNW ranges from 14.38 to 20.60 μg for *Gs. ruber* (Figure 4c); there is no correlation with fragmentation ($r = -0.1$, $P = 0.33$). During MIS M2, test weight drops initially, which is not due to increased dissolution as fragmentation is lowest during MIS M2. After this initial drop, SNW increases relative to pre-MIS M2. SNW and temperature are not correlated across the record ($r = 0.09$, $P = 0.42$) or during MIS M2 ($r = 0.19$, $P = 0.33$). High SNWs are observed at the lowest temperatures during MIS M2 at Site 999 (Figure 4c), while warming results in the lower SNW. There is a long-term trend of heavier SNW, from 3.26 to 2.9 Ma, accompanying the warming following the peak glacial in MIS M2. Both temperature and SNW remain relatively stable after MIS M2.

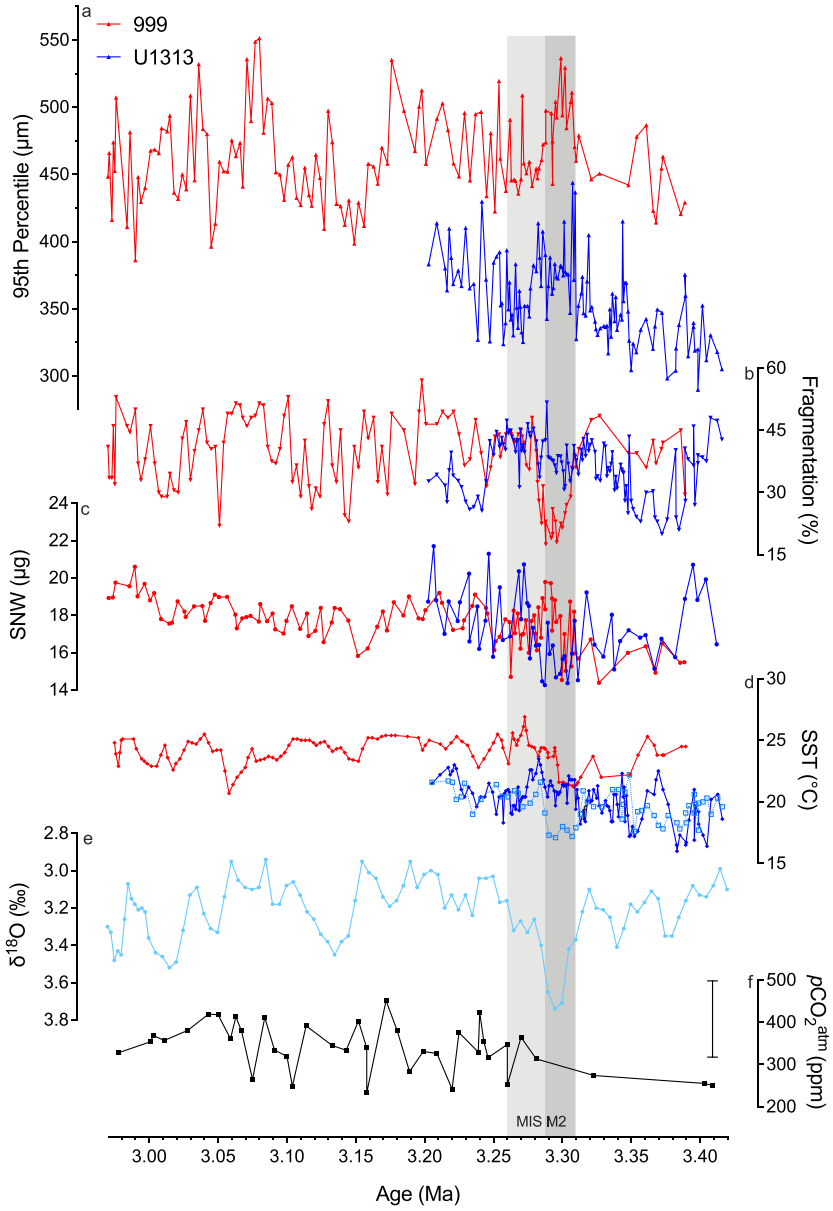

Figure 4. Plot of (a) 95th percentile of the maximum diameter (µm) of all planktic foraminifera in the assemblage; (b) planktic foraminiferal fragmentation (%); high values indicate more dissolution; (c) size-normalized weight for planktic foraminifera *Gs. ruber* for Site 999 and *G. bulloides* for Site U1313, this study (87 and 49 data points respectively), and Davis et al. (2013; 24 and 7 data points, respectively) compared with (d) solid lines: sea surface temperature (°C) from Mg/Ca for both sites (De Schepper et al., 2013; Groeneveld, 2005) and dashed blue line: alkenone sea surface temperature (°C) for Site U1313 (De Schepper et al., 2013); (e) LR04 benthic foraminifera oxygen isotope ($\delta^{18}O$ [‰]) stack (Lisiecki & Raymo, 2005); and (f) pCO_2^{atm} (ppm) reconstructed from boron isotope data from Ocean Drilling Program (ODP) Site 999; the average error bar is indicated (Bartoli et al., 2011; Martínez-Botí et al., 2015). The light grey bar indicates MIS M2 (3.26 to 3.31 Ma), and the darker grey bar indicates intense glaciation (3.285 to 3.305 Ma; De Schepper et al., 2013).

At Site U1313, SNW ranges from 14.26 to 21.70 µg for *G. bulloides* (Figure 4c), with no correlation with fragmentation ($r = -0.08$, $P = 0.54$). SNW and both Mg/Ca SST and alkenone SST are not correlated across the Pliocene ($r = -0.23$, $P = 0.12$; $r = 0.004$, $P = 0.98$), although test weight is generally lower at cooler temperatures (Figure 4b). Fragmentation increases during this period but is not correlated with SNW ($r = -0.11$, $P = 0.34$; Figure 4b). Both temperature and SNW fluctuate before and after the glacial period by 4.5 °C and 4.46 µg and 6.5 °C and 6.20 µg, respectively.

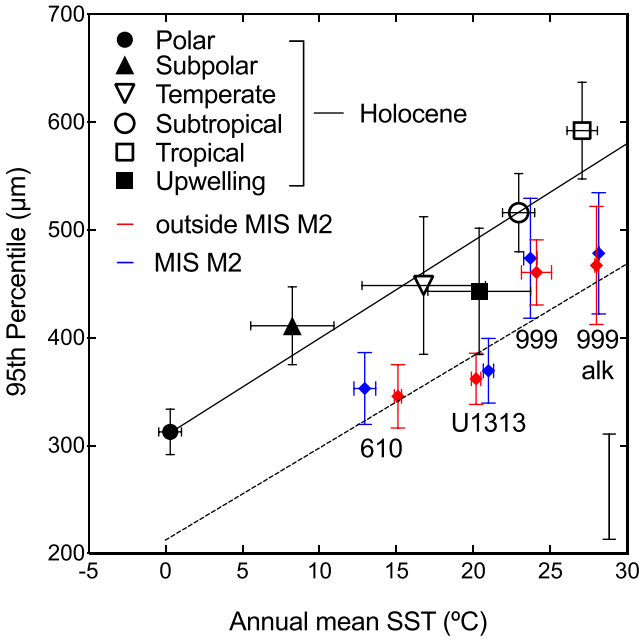

Figure 5. Holocene and Pliocene mean of the 95th percentile of assemblage size (µm) per biogeographic area plotted against sea surface temperature (SST; °C). The error bars represent the 95 % confidence intervals. The black solid line corresponds to the regression line ($r = 0.938$, $P = 0.006$) for the Holocene, using mean annual SST (Schmidt, Renaud, et al., 2004). The black dashed line indicates the trends though the new late Pliocene. Late Pliocene SST is determined as the average values: the blue symbols represent sample within MIS M2, and red symbols represent sample outside MIS M2 from Figure 4, see references for the temperature data in Figure 3 and section 2. All sites are plotted using Mg/Ca, with the exception of "999 alk," which uses alkenone SST. The black scale bar on the right of the graph represents the offset of the late Pliocene average assemblage size to the low-resolution data from Schmidt, Renaud, et al. (2004).

To better understand drivers of SNW, we analyzed CV ratios of *Gs. ruber*, the dominate species at Site 999. CV ratios during the Pliocene (Figure 6) show more calcite per volume during MIS M2 with averages of 46 % than compared to 40.3 % before MIS M2 and 41.0 % after.

4. Discussion

Planktic foraminifers strongly respond to their environment as they cannot regulate their temperature and are passively transported by ocean currents. As such they are an ideal group to study past records of climate change. Reconstructing biotic response, though, will always be hampered by our inability to describe the complex marine system with multiple drivers of change in its entirety. Carbonate chemistry is rather stable throughout the late Pliocene based on low-resolution measurements, though a higher frequency variability would be expected in analogy to Pleistocene glacial-interglacial cycles (Jansen et al., 2007; Siegenthaler et al., 2005). Therefore, our discussion focuses on the physical environment, specifically temperature and stratification, and its impact on size in the entire community of foraminifers and weight in the species *Gs. ruber* and *G. bulloides*. Based on our understanding of modern drivers of changes in size and weight in foraminifers, we would expect to see large changes in assemblage size in more variable environments and lower shell weight in lower saturation regions and time intervals where the physiological stress is strongest. Due to the evolutionary offset in size over the Neogene, assemblage size in the Pliocene should be recognizably smaller than today and increase toward the tropics.

$Size^{95/5}$ at Site 999 shows high-frequency variability throughout the Pliocene that is not related to temperature, which remains relatively stable through the study period (Groeneveld, 2005). Overall, there is little temperature change over a significant size change with cooler MIS M2 temperatures associated with the largest sizes (Figure 7). As mentioned in the methods, the Mg/Ca temperature record at this site is biased toward cooler temperatures and thus might not faithfully surface temperatures. Generally, higher fragmentation is associated with warmer temperatures as expected if warmer temperatures are related to higher pCO_2^{atm}. While preservation increases during MIS M2 at Site 999 (Figure 4), there is no correlation between fragmentation and size. This suggests that there is no bias via selectivity removing fragile larger species such as *T. sacculifer* and *Gs. ruber* nor many small fragments biasing the size data. Additionally, although there is increased fragmentation, it does not overprint our weight signal, as no signs of dissolution are observed in the CT data obtained for SNW (Figure 6; see section 3). Consequently, we interpret larger sizes and weight to reflect a biotic response, rather than a reduction of dissolution biasing the signal (see section 3).

Counterintuitively, the coldest and warmest temperatures at this location have been reconstructed during MIS M2. It is important to note that this is not a global signal but reflects the local conditions, which possibly highly sensitive to intermittent exchange between the Atlantic and Pacific Oceans in the final stages of the closure of the CAS (Bartoli et al., 2005; Haug & Tiedemann, 1998a). At this location, cooling starts before MIS M2 at 3.32 Ma and warming starts during the peak glaciation. De Schepper et al. (2013) interpreted the warming as the result of a sea level drop at the peak glaciation of MIS M2, which stopped the influx of cold Pacific water into the Caribbean.

The amplitude of size change at Site 999 is larger than at Site U1313 with a maximum change of 165 µm versus 154 µm, respectively. In contrast to Site 999, Site U1313 size is positively correlated with temperature with an increase in $size^{95/5}$ tracking the warming throughout the record (Figure 7). Alkenone SST suggests a cooling during MIS M2 at Site U1313, which is not apparent in the *G. bulloides* Mg/Ca SST, which reflect mixed layer temperatures. The surface warming corresponds with the increase in $size^{95/5}$

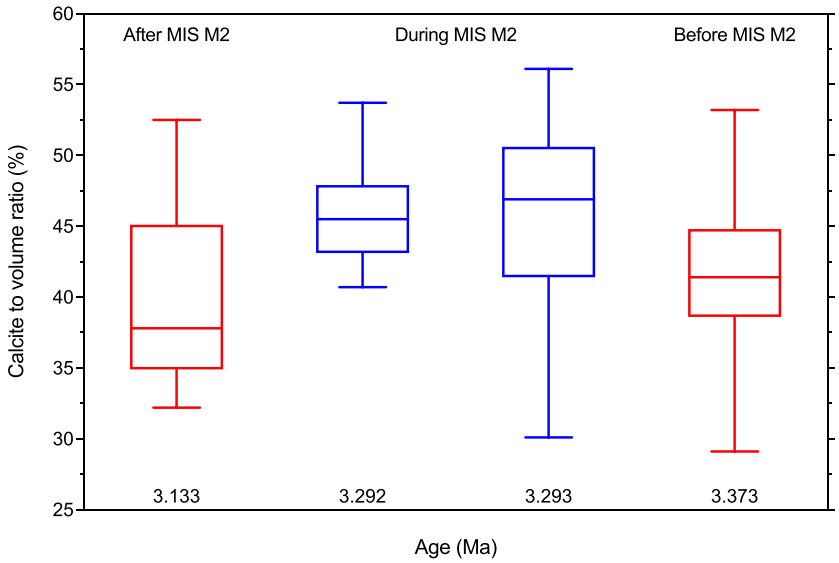

Figure 6. Drivers of change in calcification: calcite to volume ratio (%) of *Gs. ruber* from both warm samples (red), before and after MIS M2 (3.133 and 3.373 Ma), and cold samples (blue; 3.292 and 2.293 Ma) during MIS M2 in the late Pliocene. Samples are from Site 999.

implying that temperature is the dominant control on assemblage size at this site. It is unclear what has caused the divergence between the two SST proxies, but it is possible that a different genotype of *G. bulloides* has been used to produce the Mg/Ca SST record (Darling et al., 2003; De Schepper et al., 2013). It is thought that *G. bulloides* type IId has a different environmental preference from the other genotypes (Darling et al., 2003), but it is not thought to be found at Site U1313 (Kucera & Darling, 2002), where there is potential for mixing of the warm and cool water genotypes (Darling et al., 2003; Darling & Wade, 2008). However, there are no high-resolution alkenone records available for Site 999 to compare to Site U1313. Temperature records though for Site U1313 show a warming at the end of the glacial MIS M2, which is attributed to the weakening of the Atlantic Meridional Ocean Circulation (AMOC), causing a deepening of the thermocline and surface warming (Karas et al., 2017; Steph et al., 2006; Steph et al., 2010).

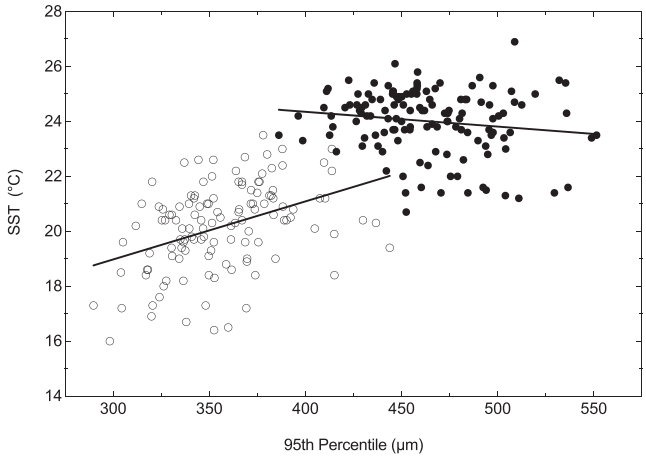

Figure 7. Plot of size versus Mg/Ca temperature at both Site 999 (closed circles) and Site U1313 (open circles) across the Pliocene. The line of regression for Site 999 shows a negative correlation between size and temperature with no statistical significance ($r = -0.15$, $P = 0.08$), whereas the line of regression for Site U1313 shows a statistically positive correlation ($r = 0.40$, $P < 0.001$).

Changes in foraminiferal assemblage size can be driven by changes in species diversity and by changes in size of the dominant species. A multitude of ecological conditions have been linked to size changes in planktic foraminifera, including pCO_2, SST, stratification, salinity, and nutrient levels (Schmidt, Thierstein, & Bollmann, 2004).

Changes to species abundance and extinctions of larger species are also important for size variation. Throughout the late Pliocene, the foraminiferal assemblage at Site 999 is affected by changes in species, either by extinction or fluctuations in occurrence (Berggren, 1969; Chaisson & Hondt, 2000). *Dentoglobigerina altispira* (3.1 Ma) and many of the *Neogloboquadrina* species go extinct (Chaisson & Hondt, 2000) in the late Pliocene. Fluctuations in the abundance of menardellids, *Neoglobquadrina dutertrei*, *Globigerinita glutinata*, *Gs. ruber*, *T. sacculifer*, and the *Globoturborotalia* group are observed (Chaisson & Hondt, 2000), all of which will impact the sizes ranges within the assemblages. Throughout the record, Site 999 is dominated by species of the *Globigerinoides*, *Trilobatus*, and *Menardella* genera, all are of the largest extant planktic foraminifers. The extant species of these groups have optimal growth conditions at temperatures between 25 and 28 °C. The

minor temperature changes between 21 and 25 °C documented for this site in the late Pliocene might therefore not lead to large changes in the size of individual species (Schmidt et al., 2006; Schmidt, Renaud, et al., 2004). However, the higher alkenone SST at ~28 °C (Bartoli et al., 2011; Martínez-Botí et al., 2015) brings the temperature closer to the optimal growth conditions, which could lead to individual size changes. Additionally, warming may lead to increases in size due to increases in abundance of *Trilobatus* over *Globigerinoides* when temperatures and salinities become closer to their species optima.

Furthermore, light availability might impact size of symbiont bearing species and their ability to thrive in these settings. The impact of light on foraminiferal assemblage composition and size has been first assessed by Ortiz et al. (1995) for the California upwelling system. They showed that high turbidity reduces light availability and thereby reduces size in symbiont-bearing species. The high productivity and resulting low light levels increase the abundance of nonsymbiont bearing species such as *G. bulloides*, which has typically smaller sizes than *Gs. ruber* and *T. sacculifer*, thereby decreasing overall sizes in the assemblage (Ortiz et al., 1995). Light availability could therefore contribute to size changes at Site 999, considering the likely changes in the position of the thermocline due to stratification changes throughout the Pliocene.

Site U1313 contains a mixture of warm water species such as *Gs. ruber* and intermediate and cold-water species such as *G. bulloides*, *Globigerina falconensis*, and *Neogloboquadrina incompta* (Channell et al., 2006). The dominant species in the analyzed time interval are *G. bulloides*, *N. incompta*, *Gt. glutinata*, and *Globrotalia hirsta*. *G. bulloides* sizes, for example, react to environmental change but show no overall net increase during this time period (Malmgren & Kennet, 1978). On contrast, a size increase of ~75 μm in *N. pachyderma* has been described for the past 1.3 Ma in the subarctic and temperate North Atlantic (Huber et al., 2000). Large-temperature fluctuations due to migration of the frontal systems led to a high variability in assemblage size in the Pleistocene (Schmidt et al., 2003). The variability of the North Atlantic Current is expressed in a dinoflagellate cyst assemblage shift and supported by both Mg/Ca and alkenone SST reconstructions for this site of 16 to 23°C (De Schepper et al., 2013; Naafs et al., 2010), and modeling outputs (Haywood et al., 2016). Both assemblage composition and size of individuals would be predicted to change in response; warming leads to an increase in abundance of *Gs. ruber* and *T. sacculifer*, which are generally larger than *G. bulloides*, *G. falconensis*, and *N. incompta* (Schmidt, Renaud, et al., 2004). Additionally, the size of the colder water species would decrease further away from their optimum, while the size of the warm water species would increase. In the Holocene, samples recovered from near frontal systems are additionally smaller than expected from the global temperature size trend (Schmidt, Renaud, et al., 2004).

Higher amplitudes of warming result in large size change in both the Pleistocene (Schmidt et al., 2003) and the Pliocene. The amplitude of warming scales with size across time, suggesting that the drivers of assemblage size in the Pleistocene were the same in the Pliocene and as such have predictive power across the entire time interval. In the Pleistocene, size changes of ~100 μm are evoked by a 10 °C change in temperature at Site GeoB1105 (1°39.9′S, 12°25.7′W, 3,225 m water depth; Schmidt et al., 2003) and ~25 μm by a 2.5 °C temperature change at the subtropical gyre Site GeoB1413 (15°40.8′S, 9°27.3′W, 3,789 m water depth; Schmidt et al., 2003). From the relationship between assemblage size and temperature shown in Figure 5, a size change of ~80 μm is associated with a 5°C change in temperature at Site 999 and ~70 μm with a 5 °C change at Site U1313. This relationship indicates that the link between foraminiferal size and palaeoclimatic fluctuations holds throughout the last 3 Myr despite changes in composition of assemblages over time, although not at the same level: over time, the increase in size is lower with the same change in temperature.

A comparison of the Pliocene planktic foraminiferal size and temperature relationship to the Holocene (Figure 5) is tentative due to the low number of sites in the Pliocene. Our dataset points to a significant difference between these time intervals, however, as Pliocene samples are significantly smaller than those in the Pleistocene. In the tropics Pliocene foraminifera are ~50 to 100 μm smaller than modern specimens at the same SST (~490 to 550 μm in the late Pliocene to ~540 to 600 μm today). This offset of around 100 μm agrees with a much lower resolution record covering the entire Cenozoic by Schmidt, Renaud, et al. (2004). The large species still dominating today's assemblages in the tropics are the same as those at 3 Ma. The observed increase in assemblage size today compared to the Pliocene is either an increase in relative abundance of the largest species such as *Globorotalia menardii* and *Globorotalia tumida*, due to increased temperature (Mary & Knappertsbusch, 2013), an increase in their size through time as documented for the latter species (Malmgren et al., 1983; Schmidt et al., 2016), or a combination of both.

The size of foraminifera at Site U1313 is smaller than expected based on the general temperature size relationship. A similar negative divergence is also observed at modern sites with high-temperature variabilities (Figure 5). While we would have expected a smaller difference in size at Site 610 given the stability of the higher latitude size records over the Cenozoic, we are reluctant to interpret the data further due to the low number of sites analyzed. There is evidence that the Pliocene equator to pole temperature gradient was lower as a result of the warmer world (Dowsett et al., 2010; Salzmann et al., 2008)) and as such might be an underling reason for this difference combined with other factors such as stronger exchange of species at the tropical site and a relative increase in size of existing species combined with a polar amplification of warming, resulting in relatively warmer temperatures in midlatitudes and little warming in the tropics (Haywood et al., 2016).

Similar to the size data, the SNW data need to be considered within a global and a local framework. In both modern and geological field studies of a variety of species, multiple drivers of weight change are indicated. In general, calcification is energetically more difficult outside optimum CO_2 conditions for each species (de Nooijer et al., 2009; Foster et al., 2013; Henehan et al., 2017) and at lower carbonate ion concentrations (Kroeker et al., 2010). In laboratory experiments, a clear reduction of weight in response to lower carbonate ion changes is documented (Beer et al., 2010; Bijma et al., 1999; Bijma et al., 2002; Henehan et al., 2017; Lombard et al., 2010; Russel et al., 2004). A reduced shell mass by up to 50% in response to increased CO_2, and therefore decreased $CO^2{}_3{}^-$, was related in both recent field studies (Henehan et al., 2017; Moy et al., 2009; Osborne et al., 2016) and over a broad geological timescale (Barker & Elderfield, 2002; Gonzalaz-Mora et al., 2008; Naik et al., 2010). The higher Pliocene CO_2 may therefore have resulted in lower calcification, thinner and/or smaller tests.

Yet Weinkauf et al. (2016, 2013) and de Moel et al. (2009) found that temperature, upwelling, productivity, and optimum growth conditions influence weight, regardless of changes in $CO^2{}_3{}^-$. Weinkauf et al. (2016) suggests that temperature and productivity control SNW in modern *Gs. ruber* with temperature increasing weight and productivity decreasing it. In contrast to Barker and Elderfield (2002), Weinkauf et al. (2016) did not find any environmental control on SNW in *G. bulloides* from the sediment core NEAP 8K in the Northeast Atlantic (59°48′N 23°54′W; water depth, 2,360 m). Gonzalaz-Mora et al. (2008) found lower SNW in *Gs. ruber* at low CO_2 and low temperature during MIS 7 in the Mediterranean, while for G. *bulloides* in the same samples, a high weight is correlated with low CO_2 and low temperatures, supporting Barker and Elderfield (2002). This led to the suggestion that the relationship between atmospheric CO_2 and weight of foraminiferal tests is species-specific and varies with location and environment, with some species showing no sensitivity at all (Davis et al., 2013; Henehan et al., 2017). Overall, there appears to be no consensus on foraminiferal calcification response to changes in CO_2, and many species responses are unknown.

These local interpretation and species-specific interpretation of drivers of calcification complicate the interpretation of SNW. SNW of *Gs. ruber* at Site 999 is heavier during the glacial interval. There is a large stepwise increase in SNW during MIS M2, parallel to warming which is interpreted as a reduction of influx of low saturation waters from the Pacific, as there is no correlation between SNW and temperature. Thus, our data may be suggesting that calcification is being controlled by a factor other than pCO_2 or that this location is not in equilibrium with the atmosphere. Today, the location reflects atmospheric conditions (Takahashi et al., 2014), but an influx of Pacific waters in the earlier part of the record, which is subsequently cut off due to eustatic sea level change at the peak of MIS M2 (De Schepper et al., 2013), would result in higher CO_2 and lower carbonate ion concentration due to the influx of upwelled waters in the earlier part of the record. Before MIS M2, we observe an overall lower SNW in *Gs. ruber* than after MIS M2 (Figure 4c), which would support an impact of carbonate ion on SNW in *Gs. ruber* in response to the local conditions.

In contrast, the SNW of *G. bulloides* at Site U1313 shows a large drop during the initial stages of MIS M2, which is a period of warming SST at U1313, although there is no correlation between temperature and SNW. The lower SNW during MIS M2 could therefore either point toward lower pH and carbonate ion concentrations and higher CO_2 during MIS M2 or link to higher energetic needs at warmer temperatures impacting calcification in the species as suggested by Davis et al. (2017) for the same location. Weight increases strongly at 3.27 Ma following the SST rise and therefore infers a decrease in calcification during warmer temperatures and thus potentially higher CO_2 in *G. bulloides*. These findings agree

with SNW for Pleistocene glacial-interglacial by Barker and Elderfield (2002) on the same species in the same region.

In our investigation of CV changes in *Gs. ruber* from Site 999, we found lower calcite volume, but higher test volume, during interglacial periods. This suggests that intervals with the coldest temperatures, more poorly ventilated waters, and higher productivity at this site (De Schepper et al., 2013; Haug & Tiedemann, 1998a; Osborne et al., 2019) are the least suitable conditions for calcification. We interpret this as a higher production of carbonate in *Gs. ruber* at lower CO_2. During MIS M2, calcite increased while volume decreased compared to samples before and after MIS M2 despite narrowly selecting for size. Furthermore, no holes or internal changes to the inner shell were observed in the CT images, which are expected in specimens that have undergone the first stages of dissolution. These findings suggest that growth and calcification are affected in different ways. *Globigerinoides ruber* has significant morphological variability, and morphotypes are known to have differing ecological preferences (Bonfardeci et al., 2018; Steinke et al., 2005). While the narrowly defined sensu stricto morphotypes were picked (see section 2.2.3), there is still some morphological variation within the specimens, which may impact the overall volume of the specimen analyzed.

Assuming similar drivers for size and weight changes, we compare amplitudes of environmental change and biotic response. Over the last 50,000 years, pCO_2 varied by 100 ppm, and SNW in *G. bulloides* ranged between 10 and 21 μg (Barker & Elderfield, 2002). In the Pliocene, SNW ranges between from 14 to 21 μg with a 40-ppm change in pCO_2 (Martínez-Botí et al., 2015), suggesting that given the error with the reconstruction and our lack of mechanistic understanding, the responses to multiple stressors are comparable.

5. Conclusions

Planktic foraminiferal assemblage size data during the late Pliocene are smaller than current sizes as expected from previous low-resolution work. Size does not respond to pCO_2 at the available resolution. Local environments are fundamental to size changes as indicated by assemblage size at Site 999, which is impacted by changes in surface ocean circulation and the intermittent influx of fresher, cooler, and more productive Pacific waters into the region in the final stages of the closure of the CAS. While a general increase in size tracks warming throughout the Pliocene, there is little response to the cooling across MIS M2 at Site U1313, whereas assemblage size at Site 999 increases. We interpret our preliminary data of overall smaller assemblage size during the Pliocene and the flatter size gradient between the tropics and poles in the late Pliocene as combination of size increases within species, changes in species composition and environmental gradients during the Pliocene.

Globigerinoides ruber and *G. bulloides* SNW show the complexity of drivers of foraminiferal weight. While there is a clear correlation between temperature and weight, our results show the importance in interpreting weight records in light of the local environments. Combining size and computer tomography analysis will have the potential to link physiological processes to changes in surface and volume of the organism and might shed light on the multiple drivers of SNW. The low glacial-interglacial variability in size-normalized weight during the Pliocene suggests that the rate or amplitude of change over glacial-interglacial periods may have a pronounced impact on the response of planktic foraminiferal calcification.

Our results would tentatively suggest that larger increases in pCO_2 result in a greater decline in calcification; higher resolution pCO_2 records across the late Pliocene would be needed to full corroborate this.

Acknowledgments
This work would not have been possible without the efforts of the ODP and IODP programs. The work was funded by NERC grant NE/P019439/1 and ERC grant ERC-2013-CoG-617303. D. N. S. was supported by a Royal Society Wolfson Merit Award. Funding for M. M. R. was provided by the U.S. Geological Survey Land Change Science Program through the PRISM4 (Paleoclimate Data Model Synergy) Project. The author would like to thank Harry Dowsett, Research Geologist at the U.S. Geological Survey, for constructive criticism of the manuscript. Any use of trade, firm, or product names is for descriptive purposes only and does not imply endorsement by the U.S. Government. A further thank you to Howard Spero and an anonymous reviewer for the constructive criticism and feedback of the manuscript. The data supporting the conclusions can be obtained from https://doi.pangaea.de/10.1594/PANGAEA.897346 and https://doi.org/10.5523/bris.3lbtbqkrrttgu1zm0orabbd67m.

References

Archer, D. E. (1996). An atlas of the distribution of calcium carbonate in sediments of the deep sea. *Global Biogeochemical Cycles*, *10*(1), 159–174. https://doi.org/10.1029/95GB03016

Aurahs, R., Treis, Y., Darling, K. F., & Kucera, M. (2011). A revised taxonomic and phylogenetic concept for the planktonic foraminifera species *Globigerinoides ruber* based on molecular and morphometric evidence. *Marine Micropaleontology*, *79*(1-2), 1–14. https://doi.org/10.1016/j.marmicro.2010.12.001

Barker, S., & Elderfield, H. (2002). Foraminiferal calcification response to glacial-interglacial changes in atmospheric CO_2. *Science*, *297*(5582), 833–836. https://doi.org/10.1126/science.1072815

Bartoli, G., Honisch, B., & Zeebee, R. E. (2011). Atmospheric CO_2 decline during the Pliocene intensification of Northern Hemisphere glaciations. *Paleoceanography*, *26*, PA4213. https://doi.org/10.1029/2010PA002055

Bartoli, G., Sarnthein, M., Weinelt, M., Erlenkeuser, H., Garbe-Schönberg, D., & Lea, D. W. (2005). Final closure of Panama and the onset of northern hemisphere glaciation. *Earth and Planetary Science Letters*, *237*(1), 33–44. https://doi.org/10.1016/j.epsl.2005.06.020

Beer, C. J., Schiebel, R., & Wilson, P. A. (2010). Testing planktic foraminiferal shell weight as a surface water [$CO^2_3{}^-$] proxy using plankton net samples. *Geology*, *38*(2), 103–106. https://doi.org/10.1130/G30150.1

Berger, W. H. (1970). Planktic foraminifera: selective solution and the lysocline. *Marine Geology*, *8*, 111–138. https://doi.org/10.1016/0025-3227(70)90001-0

Berggren, W. A. (1969). Rates of evolution in some cenozoic planktonic foraminifera. *Micropaleontology*, *15*(3), 351–365. https://doi.org/10.2307/1484931

Bijma, J., Faber, W. W. Jr., & Hemleben, C. (1990). Temperature and salinity limits for growth and survival of some planktonic foraminifers in laboratory cultures. *Journal of Foraminiferal Research*, *20*(2), 95–116. https://doi.org/10.2113/gsjfr.20.2.95

Bijma, J., Honisch, B., & Zeebe, R. E. (2002). Impact of the ocean carbonate chemistry on living foraminiferal shell weight: comment on "Carbonate ion concentration in glacial-age deep waters of the Caribbean Sea" by W. S Broecker and E. Clark. *Geochemistry, Geophysics, Geosystems*, *3*(11), 1064. https://doi.org/10.1029/2002GC000388

Bijma, J., Spero, H. J., & Lea, D. W. (1999). Reassessing foraminiferal stable isotope geochemistry: Impact of the oceanic carbonate system (experiment results). In G. Fischer, & G. Wefer (Eds.), *Uses of Proxies in Paleoceanography: Examples from the South Atlantic* (pp. 489–512). Berlin-Heidelberg: Springer Verlag. https://doi.org/10.1007/978-3-642-58646-0_20

Bollmann, J., Quinn, P., Vela, M., Brabec, B., Brechner, S., Cortes, M. Y., et al. (2004). Automated particle analysis: calcarous microfossils. In P. Francus (Ed.), *Image analysis, sediments and paleoenvironments* (pp. 229–252). Dordrecht, The Netherlands: Kluwer Academic Publishers. https://doi.org/10.1007/1-4020-2122-4_12

Bonfardeci, A., Caruso, A., Bartolini, A., Franck, B., & Blanc-Valleron, M.-M. (2018). Distribution and ecology of the *Globigerinoides ruber-Globigerinoides elongatus* morphotypes in the Azores region during the late Pleistocene-Holocene. *Paleogeography, Palaeoclimatology, Palaeoecology*, *491*, 92–111. https://doi.org/10.1016/j.palaeo.2017.11.052

Boyce, D. G., Lewis, M. R., & Worm, B. (2010). Global phytoplankton decline over the past century. *Nature*, *466*(7306), 591–596. https://doi.org/10.1038/nature09268

Caromel, A. G. M., Schmidt, D. N., Fletcher, I., & Rayfield, E. J. (2015). Morphological change during the ontogeny of the planktic foraminifera. *Journal of Micropalaeontology*, *35*, 2–19. https://doi.org/10.1144/jmpaleo2014-017

Cartapanis, O., Galbraith, E. D., Bianchi, D., & Jaccard, S. L. (2018). Carbon burial in deep-sea sediment and implications for oceanic inventories of carbon and alkalinity over the last glacial cycle. *Climate of the Past*, *14*(11), 1819–1850. https://doi.org/10.5194/cp-14-1819-2018

Chaisson, W. P., & Hondt, S. L. D. (2000). Neogene planktonic foraminifer biostratigraphy at site 999, Western Caribbean Sea. In R. M. Leckie, H. Sigurdsson, G. D. Acton, & G. Draper (Eds.), *Proceedings of the Ocean Drilling Program, Scientific Results, 165* (pp. 19–56). College Station, TX: Ocean Drilling Program. https://doi.org/10.2973/odp.proc.sr.165.010.2000

Channell, J. E. T., Kanamatsu, T., Sato, T., Stein, R., Alvarez Zarikian, C. A., Malone, M. J., & Scientists, E. (2006). Site U1313, Proceedings of the Integrated Ocean Drilling Program Expeditions 303 and 306 Scientific Prospectus. *I.O. Drilling & I. Program Management International*, *International Ocean Drilling Program, Scientific Prospectus*. College Street, TX: Integrated Ocean Drilling Program Management International, Inc.. https://doi.org/10.2204/iodp.proc.303306.112.2006

Darling, K. F., Kucera, M., Wade, C. M., von Langen, P., & Pak, D. (2003). Seasonal distribution of genetic types of planktonic foraminifer morphospecies in the Santa Barbara Channel and its paleoceanographic implications. *Paleoceanography*, *18*(2), 1032. https://doi.org/10.1029/2001PA000723

Darling, K. F., & Wade, C. M. (2008). The genetic diversity of planktic foraminifera and the global distribution of ribosomal RNA genotypes. *Marine Micropaleontology*, *67*(3-4), 216–238. https://doi.org/10.1016/j.marmicro.2008.01.009

Davis, C. V., Badger, M. P. S., Brown, P. R., & Schmidt, D. N. (2013). The response of calcifying plankton to climate change in the Pliocene. *Biogeosciences*, *10*, 6131–6139. https://doi.org/10.5194/bg-10-6131-2013

Davis, C. V., Rivest, E. B., Hill, T. M., Gaylord, B., Russell, A. D., & Sanford, E. (2017). Ocean acidification compromises a planktic calcifies with implications for global carbon cycling. *Scientific Reports*, *7*, 2225. https://doi.org/10.1038/s41598-017-01530-9

de Moel, H., Ganssen, G. M., Peeters, F. J. C., Jung, S. J. A., Kroon, D., Brummer, G. J. A., & Zeebe, R. E. (2009). Planktic foraminiferal shell thinning in the Arabian Sea due to anthropogenic ocean acidification? *Biogeosciences*, *6*, 1917–1925. https://doi.org/10.5194/bg-6-1917-2009

de Nooijer, L. N., Toyofuku, T., & Kitazato, H. (2009). Foraminifera promote calcification by elevating their intracellular pH. *Proceedings of the National Academy of Sciences*, *106*(36), 15,374–15,378. https://doi.org/10.1073/pnas.0904306106

De Schepper, S., Groeneveld, J., Naafs, D. A., Renterghem, C. D., Hennissen, J., Head, M. J., et al. (2013). Northern hemisphere glaciation during the globally warm early late Pliocene. *Public Library of Science One*, *8*(12), e81508. https://doi.org/10.1371/journal.pone.0081508

de Villiers, S. (2004). Optimum growth conditions as opposed to calcite saturation as a control on the calcification rate and shell-weight of marine foraminifera. *Marine Biology*, *144*, 45–49. https://doi.org/10.1371/journal.pone.0148363

Dowsett, H., Robinson, M., Haywood, A. M., Salzmann, U., Hill, D. J., Sohl, L. E., et al. (2010). The PRISM3D paleoenvironmental reconstruction. *Stratigraphy*, *7*, 123–139.

Dowsett, H. J., & Gill, R. P. C. (2010). Pliocene climate. *United States Geological Survey*, *7*(2-3), 106–110.

Dowsett, H. J., Robinson, M. M., & Foley, K. (2015). A global planktic foraminifer census data set for the Pliocene ocean. *Scientific Data*, *2*, 150076. https://doi.org/10.1038/sdata.2015.76

Dowsett, H. J., Robinson, M. M., Haywood, A. M., Hill, D. J., Dolan, A. M., Stoll, D. K., et al. (2012). Assessing confidence in Pliocene sea surface temperatures to evaluate predictive models. *Nature Climate Change*, *2*, 365–371. https://doi.org/10.1038/nclimate1455

Dwyer, G. S., & Chandler, M. A. (2009). Mid-Pliocene sea level and continental ice volume based on coupled benthic Mg/Ca palaeotemperatures and oxygen isotopes. Philosophical Transactions of the Royal Society A: Mathematical. *Physical and Engineering Sciences*, *367*(1886), 157–168. https://doi.org/10.1098/rsta.2008.0222

Foster, L. C., Schmidt, D. N., Thomas, E., Arndt, S., & Ridgwell, A. (2013). Surviving rapid climate change in the deep sea during the Paleogene hyperthermals. *Proceedings of the National Academy of Sciences*, *110*(23), 9273–9276. https://doi.org/10.1073/pnas.1300579110

Gonzalaz-Mora, B., Sierro, F. J., & Flores, J. A. (2008). Controls of shell calcification in planktonic foraminifers. *Quaternary Science Reviews*, *27*, 956–961. https://doi.org/10.1016/j.quascirev.2008.01.008

Groeneveld, J., (2005). Effect of the Pliocene closure of the Panamanian Gateway on Caribbean and east Pacific sea surface temperatures and salinities by applying combined Mg/Ca and $\delta^{18}O$ measurements (5.6-2.2 Ma), University of Kiel, Kiel, Germany, 161 pp.

Haug, G. H., & Tiedemann, R. (1998a). Effect of the formation of the Isthmus of Panama on Atlantic Ocean thermohaline circulation. *Nature*, *393*, 673–676. https://doi.org/10.1038/31447

Haug, G. H., & Tiedemann, R. (1998b). Stable carbon and oxygen isotope ratios of Cibicidoides wuellerstorfi, and $CaCO_3$ and sand content of ODP Hole 165-999A, Supplement to: Haug, GH; Tiedemann, R (1998): Effect of the formation of the Isthmus of Panama on Atlantic Ocean thermohaline circulation. *Nature*, *393*, 673–676. https://doi.org/10.1594/PANGAEA.789866

Haywood, A. M., Dolan, A. M., Pickering, S. J., Dowsett, H. J., Mcclymont, E. L., Prescott, C. L., et al. (2013). On the identification of a Pliocene time slice for data–model comparison. *Philosophical Transactions of the Royal Society A: Mathematical, Physical and Engineering Sciences*, *371*(2001), 20120515. https://doi.org/10.1098/rsta.2012.0515

Haywood, A. M., Dowsett, H. J., & Dolan, A. M. (2016). Integrating geological archives and climate models for the mid-Pliocene warm period. *Nature Communications*, *7*, 10646. https://doi.org/10.1098/rsta.2012.0515

Henehan, M. J., Evans, D., Shankle, M., Burke, J., Foster, G. L., Durrant, J., et al. (2017). Size-dependent response of foraminiferal calcification to seawater carbonate chemistry. *Biogeosciences*, *14*, 3287–3308. https://doi.org/10.5194/bg-14-3287-2017

Hönisch, B., Ridgwell, A., & Schmidt, D. N. (2012). The geological record of ocean acidification. *Science*, *335*, 1058–1063. https://doi.org/10.1126/science.1208277

Huber, R., Meggers, H., Baumann, K.-H., Raymo, M. E., & Henrich, R. (2000). Shell size variation of the planktonic foraminifer *Neogloboquadrina pachyderma* sin. in the Norwegian-Greenland Sea during the last 1.3 Myrs: implications for paleoceanographic reconstructions. *Palaeogeography, Palaeoclimatology, Palaeoecology*, *160*, 193–212. https://doi.org/10.1016/S0031-0182(00)00066-3

Jansen, E., Overpeck, J., Briffa, K. R., Duplessy, J.-C., Joos, F., Masson-Delmotte, V., et al. (2007). Palaeoclimate. In S. Solomon, D. Qin, M. Manning, Z. Chen, M. Marquis, K. B. Averyt, M. Tignor, & H. L. Miller (Eds.), *Climate change 2007: The physical science basis. Contribution of Working Group I to the Fourth Assessment Report of the Intergovernmental Panel on Climate Change* (pp. 444–454). Cambridge, United Kingdom and New York, N.Y., USA: Cambridge University Press.

Karas, C., Nürnberg, D., Bahr, A., Groeneveld, J., Herrle, J. O., Tiedemann, R., & deMenocal, P. B. (2017). Pliocene oceanic seaways and global climate. *Scientific Reports*, *7*, 39842. https://doi.org/10.1038/srep39842

Kroeker, K. J., Kordas, R. L., Crim, R. N., & Singh, G. G. (2010). Meta-analysis reveals negative yet variable effects of ocean acidification on marine organisms. *Ecology Letters*, *13*(11), 1419–1434. https://doi.org/10.1111/j.1461-0248.2010.01518.x

Kucera, M. (2007). Chapter Six: Planktonic foraminifera as tracers of past oceanic environments. *Developments in Marine Geology*, *1*, 213–262.

Kucera, M., & Darling, K. F. (2002). Cryptic species of planktic foraminifera: their effect on palaeoceanographic reconstructions. *Philosophical Transactions of the Royal Society A*, *360*, 695–718. https://doi.org/10.1098/rsta.2001.0962

Le, J., & Shackleton, N. (1992). Carbonated dissolution fluctuations in the western equatorial Pacific during the Late Quaternary. *Paleocoeanography*, *7*, 21–42. https://doi.org/10.1029/91PA02854

Lisiecki, L. E., & Raymo, M. E. (2005). A Pliocene-Pleistocene stack of 57 globally distributed benthic $\delta^{18}O$ records. *Paleoceanography*, *20*, PA1003. https://doi.org/10.1029/2004PA001071

Lombard, F., da Rocha, R. E., Bijma, J., & Gattuso, J. (2010). Effect of carbonate ion concentration and irradiance on calcification in planktonic foraminifera. *Biogeosciences*, *7*, 247–255. https://doi.org/10.5194/bg-7-247-2010

Lombard, F., Labeyrie, L., Michel, E., Spero, H. J., & Lea, D. W. (2009). Modelling the temperature dependent growth rates of planktic foraminifera. *Marine Micropaleontology*, *70*, 1–7. https://doi.org/10.1016/j.marmicro.2008.09.004

Malmgren, B. A., Berggren, W. A., & Lohman, G. P. (1983). Evidence for punctuated gradualism in the Late Neogene *Globorotalia tumida* lineage of planktonic foraminifera. *Paleobiology*, *9*, 377–389. https://doi.org/10.1017/S0094837300007843

Malmgren, B. A., & Kennet, J. P. (1978). Test size variation in *Globigerina bulloides* in response to Quaternary palaeoceanographic changes. *Nature*, *275*, 123–124.

Martínez-Botí, M. A., Foster, G. L., Chalk, T. B., Rohling, E. J., Sexton, P. F., Pancost, R. D., et al. (2015). Plio-Pleistocene climate sensitivity evaluated using high-resolution CO_2. *Nature*, *518*(7537), 49–54. https://doi.org/10.1038/nature14145

Mary, Y., & Knappertsbusch, M. W. (2013). Morphological variability of menardiform globorotalids in the Atlantic Ocean during Mid-Pliocene. *Marine Micropaleontology*, *101*, 180–193. https://doi.org/10.1016/j.marmicro.2012.12.001

Miller, K. G., Wright, J. D., Browning, J. V., Kulpecz, A., Kominz, M., Naish, T. R., et al. (2012). High tide of the warm Pliocene: Implications of global sea level for Antarctic deglaciation. *Geology*, *40*(5), 407–410. https://doi.org/10.1130/G32869.1

Moy, A. D., Howard, W. R., Bray, S. G., & Trull, T. W. (2009). Reduced calcification in modern Southern Ocean planktonic foraminifera. *Nature Geoscience*, *2*, 276–280. https://doi.org/10.1038/ngeo460

Naafs, B. D. A., Stein, R., Hefter, J., Khélifi, N., De Schepper, S., & Haug, G. H. (2010). Late Pliocene changes in the North Atlantic Current. *Earth and Planetary Science Letters*, *298*(3), 434–442. https://doi.org/10.1016/j.epsl.2010.08.023

Naik, S. S., Naidu, P. D., Govil, P., & Godad, S. (2010). Relationship between weights of planktonic foraminifer shell and surface water $CO_3^=$ concentration during the Holocene and Last Glacial Period. *Marine Geology*, *275*, 278–282. https://doi.org/10.1016/j.margeo.2010.05.004

National Aeronautics and Space Administration, (2019). Global climate change: Vital signs of the planet. https://climate.nasa.gov/vital-signs/carbon-dioxide/

Ortiz, J. D., Mix, A. C., & Collier, R. W. (1995). Environmental control of living symbiotic and symbiotic foraminifera of the California Current. *Paleoceanography*, *10*(6), 987–1009. https://doi.org/10.1029/95PA02088

Osborne, A. H., Hathorne, E. C., Böning, P., Groeneveld, J., Pahnke, K., & Frank, M. (2019). Late Pliocene and Early Pleistocene variability of the REE and Nd isotope composition of Caribbean bottom water: A record of changes in sea level and terrestrial inputs during the final stages of Central American Seaway closure. *Paleoceanography and Paleoclimatology*, 2019PA003654. https://doi.org/10.1029/2019PA003654

Osborne, E. B., Thunnel, R. C., Marshall, B. J., Holm, J. A., Tappa, E. J., Benitez-Nelson, C., et al. (2016). Calcification of the planktic foraminifera *Globigerina bulloides* and carbonate ion concentrations: Results from the Santa Barbara Basin. *Paleoceanography*, *31*, 1083–1102. https://doi.org/10.1002/2016PA002933

Pagani, M., Liu, Z., LaRiviere, J., & Ravelo, A. C. (2010). High Earth-system climate sensitivity determined from Pliocene carbon dioxide concentrations. *Nature Geoscience*, *3*(1), 27–30. https://doi.org/10.1038/NGEO724

Pörtner, H. O., Karl, D., Boyd, P. W., Cheung, W., Lluch-Cota, S. E., Nojiri, Y., et al. (2014). Ocean Systems. In C. B. Field, et al. (Eds.), *Climate Change: Impacts, Adaption, and Vulnerability. Part A: Global and Sectoral Aspects. Contribution of Working Group II to the 5th Assessment Report of the IPCC* (pp. 411–484). Cambridge, UK: Cambridge University Press.

Renaud, S., & Schmidt, D. N. (2003). Habitat tracking as a response of the planktic foraminifer *Globorotalia truncatulinoides* to environmental fluctuations during the last 140 kyr. *Marine Micropaleontology*, *49*, 97–122. https://doi.org/10.1016/S0377-8398(03)00031-8

Rink, S., Kühl, M., Bijma, J., & Spero, H. J. (1998). Microsensor studies of photosynthesis and respiration in the symbiotic foraminfer *Orbulina universa*. *Marine Biology*, *131*, 583–595. https://doi.org/10.1007/s002270050350

Robinson, M. M., Dowsett, H. J., & Chandler, M. A. (2008). Pliocene role in assessing future climate impacts. *Eos*, *89*(49), 501–502. https://doi.org/10.1029/2008EO490001

Ruddiman, W. F., Kidd, R. B., Thomas, E., et al. (1983). Site 610. In D.S.D. Project (Ed.), *Initial report of the Deep Sea Drilling Project* (pp. 351–470). Washington: U.S. Govt. Printing Office. https://doi.org/10.2973/dsdp.proc.94.106.1987

Russel, A. D., Hönisch, B., Spero, H. J., & Lea, D. W. (2004). Effects of seawater carbonate ion concentration and temperature on shell U, Mg, and Sr in cultured planktonic foraminifera. *Geochimica et Cosmochimica Acta*, *68*, 4347–4361. https://doi.org/10.1016/j.gca.2004.03.013

Salzmann, U., Haywood, A. M., Lunt, D. J., Valdes, P. J., & Hill, D. J. (2008). A new global biome reconstruction and data-model comparison for the Middle Pliocene. *Global Ecology and Biogeography*, *17*, 432–447. https://doi.org/10.1111/j.1466-8238.2008.00381.x

Schiebel, R. (2002). Planktic foraminiferal sedimentation and the marine calcite budget. *Global Biogeochemical Cycles*, *16*(4), 1065. https://doi.org/10.1029/2001GB001459

Schmidt, D. N., Caromel, A. G. M., Seki, O., Rae, J. W. B., & Renaud, S. (2016). Morphological response of planktic foraminifers to habitat modifications associated with the emergence of the Isthmus of Panama. *Marine Micropaleontology*, *128*, 28–38. https://doi.org/10.1016/j.marmicro.2016.08.003

Schmidt, D. N., Lazarus, D., Young, J. R., & Kucera, M. (2006). Biogeography and evolution of body size in marine plankton. *Earth Science Reviews*, *78*(3-4), 239–266. https://doi.org/10.1016/j.earscirev.2006.05.004

Schmidt, D. N., Renaud, S., & Bollmann, J. (2003). Response of planktic foraminiferal size to late Quaternary climate change. *Paleoceanography*, *18*(2), 1039. https://doi.org/10.1029/2002PA000831

Schmidt, D. N., Renaud, S., Bollmann, J., Schiebel, R., & Thierstein, H. R. (2004). Size distribution of Holocene planktic foraminifer assemblages: biogeography, ecology and adaption. *Marine Micropaleontology*, *50*, 319–338. https://doi.org/10.1016/S0377-8398(03)00098-7

Schmidt, D. N., Thierstein, H. R., & Bollmann, J. (2004). The evolutionary history of size variation of planktic foraminiferal assemblages in the Cenozoic. *Palaeogeography Palaeoclimatology Palaeoecology*, *212*, 159–180. https://doi.org/10.1016/j.palaeo.2004.06.002

Schmidt, D. N., Thierstein, H. R., Bollmann, J.ö., & Schiebel, R. (2004). Abiotic forcing of plankton evolution in the Cenozoic. *Science*, *303*(5655), 207–210. https://doi.org/10.1126/science.1090592

Seki, O., Foster, G. L., Schmidt, D. N., Mackensen, A., Kawamura, K., & Pancost, R. D. (2010). Alkenone and boron-based Pliocene pCO_2 records. *EPSL*, *292*(1-2), 201–211. https://doi.org/10.1016/j.epsl.2010.01.037

Siegenthaler, U., Monnin, E., Kawamura, K., Spahni, R., Schwander, J., Stauffer, B., et al. (2005). Supporting evidence from the EPICA Dronning Maud Land ice core for atmospheric CO_2 changes during the past millennium. *Tellus*, *57B*, 51–57. https://doi.org/10.3402/tellusb.v57i1.16774

Sigurdsson, H., Leckie, M., & Acton, G. D. (1996). Ocean Drilling Program Leg 165 preliminary report: Caribbean Ocean history and the Cretaceous/Tertiary boundary event. In H. Sigurdsson, R. M. Leckie, G. D. Acton et al. (Eds.), *Proc. ODP, Init. Repts., 165: College Station, TX (Ocean Drilling Program)* (pp. 377–400). https://doi.org/10.2973/odp.proc.ir.165.108.1997

Spero, H. J., Bijma, J., Lea, D. W., & Bemis, B. E. (1997). Effect of seawater carbonate concentration on foraminiferal carbon and oxygen isotopes. *Nature*, *390*, 497–500. https://doi.org/10.1038/37333

Steinke, S., Chiu, H.-Y., Yu, P.-S., Shen, C.-C., Lowemark, L., Mii, H.-S., & Chen, M. T. (2005). Mg/Ca ratios of two *Globigerinoides ruber* (white) morphotypes: Implications for reconstructing past tropical/subtropical surface water conditions. *Geochemistry, Geophysics, Geosystems*, *6*, Q11005. https://doi.org/10.1029/2005GC000926

Steph, S., Tiedemann, R., Groeneveld, J., Sturm, A., & Nürnberg, D. (2006). Pliocene changes in tropical East Pacific upper ocean stratification: Response to tropical gateways? In R. Tiedemann, A. C. Mix, C. Richter, & W. F. Ruddiman (Eds.), *Proceedings of the Ocean Drilling Program, Scientific Results, 202* (pp. 1–55). College Station, TX: Ocean Drilling Program. https://doi.org/10.2973/odp.proc.sr.202.211.2006

Steph, S., Tiedemann, R., Prange, M., Groeneveld, J., Schulz, M., Timmermann, A., et al. (2010). Early Pliocene increase in thermohaline overturning: A precondition for the development of the modern equatorial Pacific cold tongue. *Paleoceanography*, *25*, PA2202. https://doi.org/10.1029/2008PA001645

Takahashi, T., Sutherland, S. C., Chipman, D. W., Goddard, J. G., & Ho, C. (2014). Climatological distributions of pH, pCO_2, total CO_2, alkalinity, and $CaCO_3$ saturation in the global surface ocean, and temporal changes at selected locations. *Marine Chemistry*, *164*, 95–125. https://doi.org/10.1016/j.marchem.2014.06.004

Tan, N., Ramstein, G., Dumas, C., Contoux, C., LAdant, J.-B., Sepulchre, P., et al. (2017). Exploring the MIS M2 glaciation occurring during the warm and high atmospheric CO_2 Pliocene background climate. *Earth and Planetary Science Letters*, *472*, 266–276. https://doi.org/10.1016/j.epsl.2017.04.050

Thunnel, R. C. (1982). Carbonate dissolution and abyssal hydrography in the Atlantic. *Marine Geology*, *47*, 165–180. https://doi.org/10.1016/0025-3227(82)90067-6

Tiedemann, R. & Franz, S. O. (1997). Deep-water circulation, chemistry, and terrigenous sediment supply in the equatorial Atlantic during the Pliocene, 3.3-2.6 Ma and 5-4.5 Ma. https://doi.org/10.2973/odp.proc.sr.154.120.1997

Weinkauf, M. F. G., Kunze, J. G., Waniek, J. J., & Kucera, M. (2016). Seasonal variation in shell calcification of planktonic foraminifera in the NE Atlantic reveals species-specific response to temperature, productivity, and optimum growth conditions. *Public Library of Science One*, *11*(2), e0148363. 1-33. https://doi.org/10.1371/journal.pone.0148363

Weinkauf, M. F. G., Moller, T., Koch, M. C., & Kucera, M. (2013). Calcification intensity in planktonic foraminifera reflects ambient conditions irrespective of environmental stress. *Biogeosciences*, *10*, 6639–6655. https://doi.org/10.5194/bg-10-6639-2013

Wolf-Gladrow, D. A., Bijma, J., & Zeebe, R. E. (1999). Model simulation of the carbonate chemistry in the microenvironment of symbiont bearing foraminifera. *Marine Chemistry*, *64*(3), 181–198. https://doi.org/10.1016/S0304-4203(98)00074-7